第28卷 第4期
2007年4月

半 导 体 学 报
CHINESE JOURNAL OF SEMICONDUCTORS

Vol.28 No.4
Apr.,2007

Detection of Terahertz Photon by GaAs-Based Single Electron Transistor at Low Temperatures*

Han Weihua[1,†], Yomoto M[2], and Kasai S[2]

(1 *Research Center of Engineering for Semiconductor Integrated Technology, Institute of Semiconductors, Chinese Academy of Sciences, Beijing 100083, China*)
(2 *Research Center for Integrated Quantum Electronics, Hokkaido University, Sapporo 060-8628, Japan*)

Abstract: A reproducible terahertz (THz) photocurrent was observed at low temperatures in a Schottky wrap gate single electron transistor with a normal-incident of a CH_3OH gas laser with the frequency 2.54THz. The change of source-drain current induced by THz photons shows that a satellite peak is generated beside the resonance peak. THz photon energy can be characterized by the difference of gate voltage positions between the resonance peak and satellite peak. This indicates that the satellite peak exactly results from the THz photon-assisted tunneling. Both experimental results and theoretical analysis show that a narrow spacing of double barriers is more effective for the enhancement of THz response.

Key words: single electron transistors; THz photon detection; photon-assisted tunneling
EEACC: 2560
CLC number: TN321 **Document code**: A **Article ID**: 0253-4177(2007)04-0500-07

1 Introduction

The terahertz (THz) wave frequency region has attracted considerable attention as a remaining frequency resource for applications such as high-capacity communications, biomedical imaging, chemical analysis by molecular spectroscopy, airport security, and remote sensing in space. Low-dimensional semiconductor systems are one of most suitable candidates for working in the THz frequency regime. This is due to the fact that the conducting electrons in low-dimensional systems are confined within a nanoscale spacing, so that the quantized energies fall into the meV scale, corresponding to the THz frequency regime.

Tien-Gorden theory described the photon-assisted tunneling in superconducting tunnel junctions[1], through which the tunneling of an electron with energy E can exchange a photon energy $h\omega$ with a microwave field, creating a new set of electron states $E + nh\omega$. Based on this idea, photon-assisted quantum tunneling has been widely studied for tunnel semiconductor devices such as resonant tunneling diodes (RTD)[2], semiconductor superlattices[3], point contact devices[4], and single electron transistors (SET)[5,6]. The scale of quantized energy in such semiconductor nanostructures is comparable to the energy of a THz photon. If a THz wave couples into this kind of low-dimensional semiconductor quantum device, THz photon-assisted electrons will modify the tunnel current according to Tien-Gorden theory. The Asada research group observed the gradual current change of a triple-barrier RTD under THz irradiation from the classical square-law detection to photon-assisted tunneling with increasing THz photon energy[2]. The THz operation of the RTD was based on an inter-subband resonance and depended on the applied bias voltage producing the correct subband alignment of the two wells. In a superlattice driven by intense THz electric fields, Keay *et al*. also observed absolute negative conductance and new current steps and plateaus[3]. At low DC bias the drift of electrons in a superlattice is reduced because of the frequency modulation of the Bloch oscillation by the intense THz frequency field. At higher DC bias, the THz field opens new conduction channels in the neighboring well

* Project supported by the National Natural Science Foundation of China (No.60506017)
† Corresponding author. Email: weihua@red.semi.ac.cn
Received 6 July 2006, revised manuscript received 7 December 2006
©2007 Chinese Institute of Electronics

and the current increases, resulting in the formation of current steps. Wyss *et al*. reported that pronounced far-infrared photon-induced current ministeps could be detected by quantum point contact devices defined by split-gate electrodes[4]. The quantum point contact exhibits the current plateau behavior of a one-dimensional electron system. Incoming photons increase the energy of electrons so that electrons can travel through the opening channels in a one-dimensional gas. Many researchers have studied THz photon detection by SET. In one detection mechanism, ordinary Coulomb blockade oscillations are modified by the absorption of photons by tunneling electron[5]. Sidebands originate from matching the ground and excited states to the Fermi levels of the leads by a photon energy. Such a quantum dot detector offers the possibility to tune the discrete states of the dot easily by varying electro-static potentials, thus allowing for frequency-selective detection. Another mechanism is based on the polarization of charges in a quantum dot created by far-infrared photons, which cause the conductance resonance peaks to shift[6]. A quantum-dot single-photon detector was developed by Komiyama using a cold (50mK) SET in a high magnetic field and using double quantum dots with no magnetic field. Incident THz photons are coupled into the quantum dot via small dipole antennas. Within the quantum dot, an electron-hole pair created by the incident photon releases energy to the crystal lattices, which causes a polarization between two closely coupled electron reservoirs. Electron tunneling occurs, causing a shift in the gate voltage of the SET.

In this paper, we report the investigation of the mechanism of THz photon-assisted tunneling by means of a GaAs-based Schottky wrap-gate single electron transistor at low temperatures. A normal-incident THz laser induces a change in the source-drain current, which shows that a satellite peak generates beside the resonance peak. The THz photon energy can be characterized by the difference in gate voltage positions between the resonance peak and satellite peak.

2 Experiments

The SET devices were fabricated on a δ-doped GaAs/AlGaAs heterostructure wafer. The GaAs/AlGaAs heterostructure wafer was grown by molecular beam epitaxy and consisted of a semi-insulating GaAs substrate, a 500nm-thick buffer layer of undoped GaAs, a 100nm-thick layer of undoped $Al_xGa_{1-x}As$, $x = 0.33$, a 20nm-thick layer of undoped GaAs, a 10nm-thick layer of undoped $Al_xGa_{1-x}As$, $x = 0.33$, a δ-doped layer with carrier density $3\times10^{12}cm^{-2}$, a 50nm-thick layer of undoped $Al_xGa_{1-x}As$, $x = 0.33$, and a 10nm-thick GaAs cap layer doped with Si at $1\times10^{18}cm^{-2}$. Figure 1(a) shows a scanning electron microscope (SEM) image of the fabricated SET, which consists of a GaAs-based heterostructure nanowire surrounded by double nanoscale Schottky gates. The nanowires were patterned on top of the GaAs/AlGaAs heterostructure wafer using electron-beam lithography and a developing procedure. Isotropic wet etching in a cooling H_2SO_4 : H_2O_2 : H_2O solution was carried out to transfer the nanowire pattern onto the GaAs/AlGaAs heterostructure. The two-dimensional electron gas (2DEG) that forms at the GaAs/AlGaAs hetero-interface is located 70nm below the sample surface and has a mobility $\mu = 1.19\times10^5 cm^2/(V\cdot s)$ and sheet electron density $n_s = 6.43\times10^{11} cm^{-2}$ at a low temperature of 77K. From these data we can extract a mean free path of $l_e = 25.8\mu m$ and Fermi wavelength in the 2DEG region of $\lambda_F = 31nm$. The nanowires of the two investigated devices had widths of 680nm and 580nm, respectively. The Ohmic contact of the source and drain electrodes was fabricated by following procedures including photolithography, the evaporation of multiple metal layers Ge/Au/Ni/Au, and lift-off and annealing at 430℃. E-beam overlay exposure was used to pattern double gate stripes. The gate length is 100nm and the gate spacing is 200nm or 300nm for different devices. Metal Cr/Au deposition and lift-off procedures transfer the nanoscale gate pattern onto the nanowire mesa. Schottky barriers of about 0.7eV were formed between Cr and GaAs interface to stop leakage current. Then an SiO_2 layer with a thickness of 30nm covered the whole surface of the sample for the passivation of surface states. Finally, for electronic tests, electrode down-leads were impressed on the electrode windows of SiO_2 layer.

The devices were shielded in a vacuum test

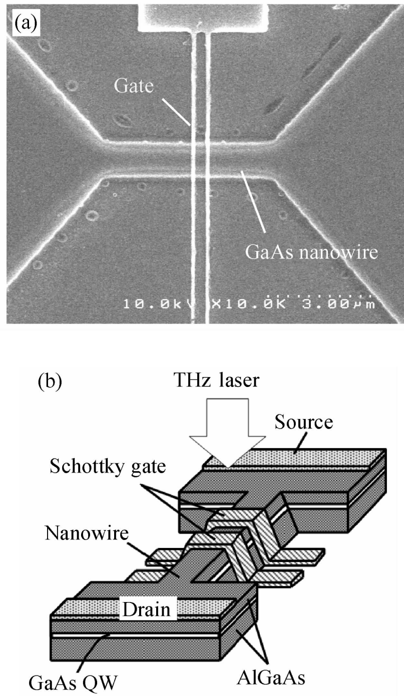

Fig. 1 (a) SEM image of a fabricated Schottky-wrap gate SET; (b) Schematic diagram of THz detection measurement by the SET

box in order to screen out disturbances from the environment. In order to avoid heating electrons by the electric field, the source/drain voltage was kept at 0.2mV, which is below $k_B T/e \approx 0.862$ mV at 10K. The current-voltage characteristics between the source-drain current and gate voltage were measured at low temperatures using an Agilent 4156C semiconductor parameter analyzer. With suitable negative voltages of double Schottky wrap gates, electrons under the gates were depleted to form a quasi-one-dimensional electron gas in a short central channel (i.e., a quantum point contact structure). Further negatively increasing the gate voltage, the electrons along the channel were pinched off completely to form double barrier potentials. Then a quantum dot was sandwiched between both barriers. The size of the quantum dot could be adjusted flexibly by double gates so that the energy level position and level spacing could be tuned effectively. The smaller the quantum dots became, the thicker double barriers needed to be. Thus only a few current peaks resulting from resonant tunneling could be observed near the pinch-off gate threshold voltage.

Figure 1(b) shows the measurement of THz detection. The detection experiments were performed by measuring the change of source-drain current with varying gate voltages in the SET at temperatures of 6～7K under the normal-incident 2.54 THz far infrared laser, which radiates from CH_3OH gas pumped by a CO_2 laser. The size of the conductive mesa is of the order of several hundred microns, comparable to a THz wavelength of 118mm. The alternate THz electric field is perpendicular to the THz wave propagation. Therefore the normal incident THz laser wave was very helpful to induce electrons confined in the nanowire and the quantum dot. By adjusting the gate voltage, the change of level spacing in the quantum dot makes tunable THz photon detection more effective. THz photocurrent response was obtained from the difference between source-drain current with and without THz laser irradiation. In order to exclude the influence of random noise, the source-drain current was measured repeatedly using a fine scanning step (0.01mV) of the gate voltage. Reproducible response results confirm that the photocurrent closely relates to the absorption of THz photons.

3 Estimation of THz photocurrent

At finite temperature, the current peak of single-electron resonant tunneling can be given by a Landauer-type formula for symmetric barriers[7],

$$I_{DS}(V_G) = G_0 V_{DS} \frac{1}{4k_B T}\int_{-\infty}^{+\infty} \cosh^{-2}\left(\frac{E}{2k_B T}\right)\times \frac{\Gamma^2}{[E - e\alpha(V_N - V_G)]^2 + \Gamma^2}\mathrm{d}E \quad (1)$$

where $G_0 = \frac{e^2}{h}A$ and A is the temperature-independent energy-integrated strength of resonance, T is the low temperature, Γ is the level broadening resulting from resonant tunneling, and V_N is the gate voltage at resonance. The scaling factor $\alpha = \Delta E/e\Delta V_G$ and quantized energy ΔE are determined by quantum level spacing $\Delta\varepsilon$ and charging energy $U = e^2/2C$ (C is the total capacitance). For sufficiently low temperatures ($\Gamma < kT < \Delta\varepsilon < U$), electron transport across the device with low source-drain bias is dominated by quantum tunneling through a single level. In this temperature range, the full width of the resonance peak at half maximum, arising from the thermal broadening of the Fermi distribution of the electrons, is linear:

FWHM $=3.52k_{B}T/e\alpha$.

The current peak line shape modified by THz photon-assisted tunneling is given by Tien-Gorden theory[1]. In this theory, n photon absorption or emission is viewed as creating a new set of electron eigenstates with energies $E+nh\omega$, where E is the eigenenergy of the original electron state without irradiation and n is a negative integer for absorption and positive integer for emission. The time dependence of the wave function for every single-electron state will be modified according to

$$\psi(x,t)=\psi(x)\exp\left[-\frac{i}{\hbar}\int^{t}dt(E+eV_{ac}\cos\omega t)\right]$$
$$=\psi(x)\sum_{n=-\infty}^{+\infty}J_{n}(eV_{ac}/h\omega)\exp[-i(E+nh\omega)t/h] \quad (2)$$

where E is the unperturbed energy of the Bloch state, J_n is the nth order Bessel function of the first kind, V_{ac} is the AC-coupling voltage, and $h\omega$ is the photon energy. The applied AC voltage is assumed to modulate adiabatically the potential energy for each quantum level, which is equivalent to DC voltages $nh\omega/e$ applied across the barrier with the probability amplitude $J_n(eV_{ac}/h\omega)e^{-in\omega t}$ for transitions between the modulated state and any unmodulated eigenstates. Thus source-drain current modulated by the absorption of THz photons can be given by

$$\tilde{I}_{DS}(V_{G})=G_{0}V_{DS}\frac{1}{4k_{B}T}\int_{-\infty}^{+\infty}\cosh^{-2}\left(\frac{E}{2k_{B}T}\right)\times$$
$$\sum_{n=-\infty}^{+\infty}\frac{J_{n}^{2}(eV_{ac}/h\omega)\Gamma^{2}}{[E-e\alpha(V_{N}-V_{G})+nh\omega]^{2}+\Gamma^{2}}dE \quad (3)$$

Therefore, a THz photocurrent can be determined from the difference between the resonance peaks with and without THz irradiation, namely,

$$\Delta I_{DS}(V_{G})=\tilde{I}_{DS}(V_{G})-I_{DS}(V_{G}) \quad (4)$$

The response of THz photocurrent might provide a kind of spectrum in both frequency and intensity of THz waves. Since the THz photocurrent is extracted from the resonance peaks of the source-drain current, the separation of the THz photocurrent is most important for the spectrum. In order to obtaining a clear spectrum, the photon-assisted tunneling must be dominant in the electron quantum transport with following challenges:

(1) The charge energy must be larger than the thermal energy ($U>k_{B}T$), because the operation of a single electron tunneling through the SET depends on the Coulomb blockade effect.

(2) The THz photon energy should exceed the level broadening (i.e. $h\omega>\Gamma$) for the electrons on the quantum dot. When the photon energy $h\omega>\Gamma$, i.e. $\omega>1/\tau$, each electron experiences at least one period of the THz signal within the mean time t tunneling through the double barriers[8]. If the THz frequency $\omega<1/\tau$, each electron on the dot hasn't gone through a period of the THz field. In this adiabatic driving regime, electrons on the dot only see an essentially static potential and cannot be induced by THz alternative electric field.

(3) A THz photocurrent might be observed clearly if the THz photon energy is larger than thermal broadening of the resonant levels $h\omega>3.52k_{B}T$[9]. However, THz photocurrents are masked by thermal broadening of levels at higher temperatures. In that case the THz photocurrents have to be extracted from the difference between source-drain current with and without THz laser irradiation.

Electrons by photon-assisted tunneling through the quantum dot can conserve both energy and momentum. The electrons that absorb THz photons will not release the THz photon energy easily by an LO-phonon due to the strong quantum confinement in the nanostructure. The LO-phonon scattering can be prohibited during the electron tunneling process from electron reservoirs to the quantum dot according to Fermi's Golden rule and the momentum selection rule.

4 Results and discussion

Reproducible THz photocurrents of two devices with different quantum dot sizes have been obtained from the difference between source-drain current with and without THz laser irradiation, as shown in Fig. 2. By comparison of the current characteristics of the two devices, both the resonant current peak and the photocurrent peak in device B are more remarkable than in device A. Table 1 shows the confinement space size of quantum dots for devices A and B by comparing the scale parameters of the nanowires and double gates. The smaller the quantum dot size, the better the device characteristics become. The improvement of local confinement in the quantum dot can

increase the level spacing and enhance the discreteness of the resonance peaks. Figure 2 indicates that the increased local confinement of the quantum dot in device B is very useful for increasing the THz response.

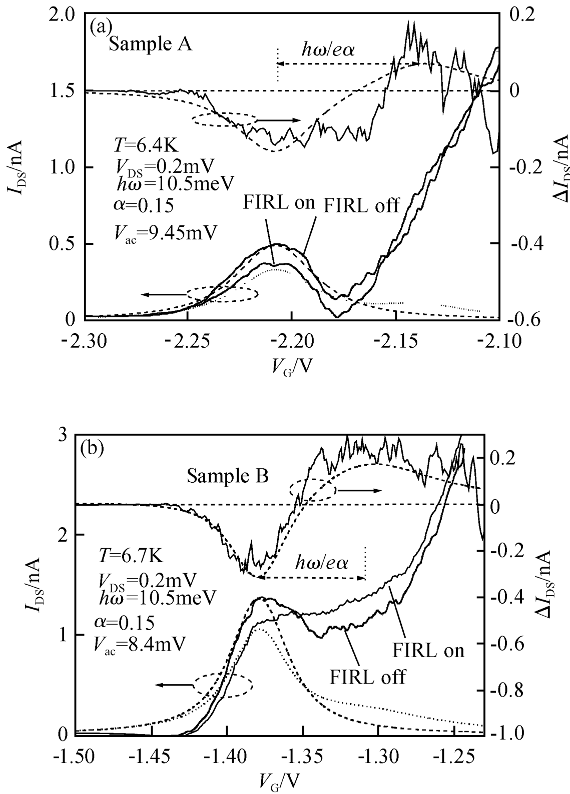

Fig.2 THz photocurrent response and source-drain currents with and without 2.525THz normal-incident far infrared laser (FIRL) irradiation for device A (a) and device B (b)

Table 1 Parameters of device structure

Device No.	Nanowire		Gate	
	Width/nm	Length/μm	Length/nm	Spacing/nm
A	680	4	100	300
B	580	4	100	200

If the photocurrent response results from the THz laser irradiation, the gate voltage difference ($\Delta V_{Gp}=70$mV for both devices) between the resonance peak and satellite peak should be sufficient to characterize THz photon energy (10.5meV), i.e. $h\omega=\alpha e\Delta V_{Gp}$. In order to prove this assumption, a source-drain current with THz irradiation was simulated by Tien-Gorden theory for both devices. The simulated current curves agreed well with the characteristics of the experimental source-drain current. From the curve fitting process, we obtained the same scaling factor $\alpha=0.15$ for both devices. This value of the scaling factor is just what we hoped. Since the scaling factor is related to gate capacitance and total capacitance, the same scaling factor α indicates that both devices with the same gate length have similar gate depletion layers.

The scaling factor α is very important for the scale of the THz photon energy. The experiment on the temperature dependence of the resonance peaks in sample A was done for the verification of the scaling factor. The measured conductance characteristics as a function of temperatures are shown in Fig.3(a). With the increase of temperature, the resonant current peak width is basically broadened as $(\Gamma+3.52k_BT)/\alpha e$ in Fig.3(b). The level broadening of the resonance peak is $\Gamma=3$meV, which is extracted from the curve fitting process. The scaling parameter α was estimated to be 0.146 at 6.4K. This indicates that the satellite peak was exactly generated by THz photons.

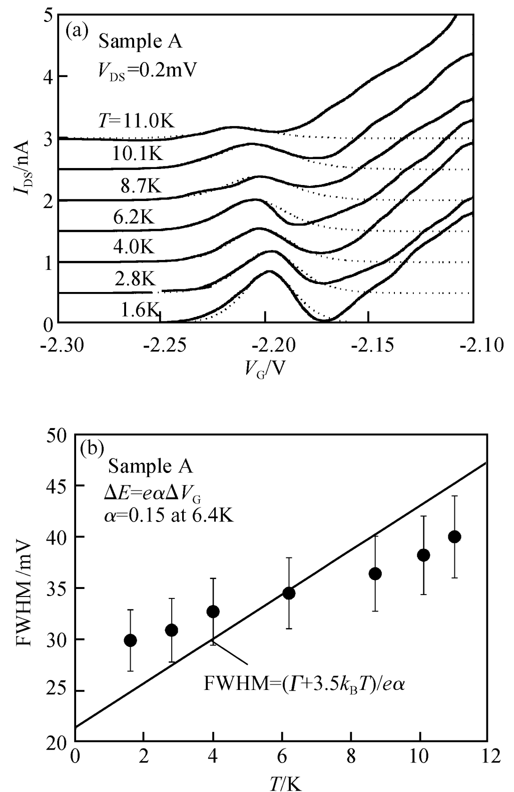

Fig.3 Temperature dependence of current peak (a) and their full width at half maximum (FWHM)(b)

In order to develop the SET into a THz photon detector operating at higher temperature, the

theoretical temperature dependences of the THz photocurrent for device B with smaller quantum dots are shown in Fig. 4. We have noticed that the THz photocurrent is sensitive to the resonant level broadening Γ and THz voltage V_{ac}. The THz photocurrent peak might persist up to room temperature if Γ and V_{ac} are suitable. Figure 4 (a) shows that the THz photocurrent height is increased when $eV_{ac}/\hbar\omega<2$. The THz voltage could be adjusted by input power ($V_{ac}\propto\sqrt{P_{in}}$). Figure 4(b) indicates that the increase of the resonant level broadening Γ is useful for the improvement of the THz photocurrent response at higher temperature.

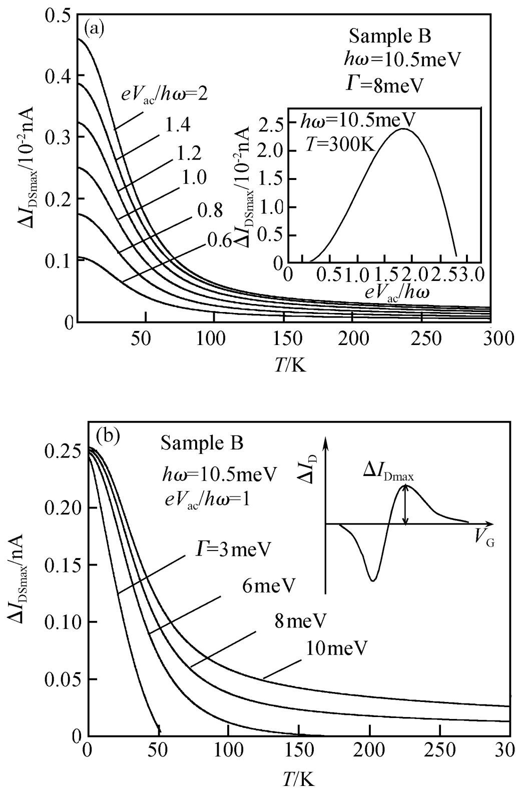

Fig. 4 Temperature dependence of simulated THz photocurrent amplitude

For a symmetric double barrier structure, the resonant level broadening Γ depends not only on the double barrier spacing but also the barrier thickness and height, namely

$$\Gamma=\frac{\hbar}{\tau_d}\approx\frac{4\hbar}{\tau_r}\exp\left(-2\int_0^w\sqrt{2m^*(\phi(x)-E_r)/\hbar^2}\,dx\right) \quad (5)$$

where τ_d is the dwell time, w is the barrier thickness, $\phi(x)$ is the barrier height, E_r is the resonance energy, and m^* is the effective electron mass. The return time τ_r of a electron reflecting between barriers is determined by barrier spacing a and electron velocity:

$$\tau_r = a\sqrt{\frac{2m^*}{E_r}} \quad (6)$$

Assuming quantum dot as a box with area a^2, the p-th state $E_p=\frac{\hbar^2\pi^2p^2}{2m^*a^2}$ ($p=1,2,3\cdots$). If $E_r=E_p$, then

$$\tau_r = \frac{2a^2m^*}{p\hbar\pi} \quad (7)$$

Therefore increasing Γ mainly requires a narrower barrier thickness and shorter barrier spacing. The experiment results in Fig. 2 show that the THz photocurrent in device B with shorter barrier spacing is better than that in device A. Although a small quantum dot can increase the level broadening Γ, the dwell time of electrons on the quantum dot will be shorter than a period of a THz wave. More electrons in the nanowire would rather absorb THz photons than in the quantum dot. The discrete levels of the quantum dot will provide tunneling channels for those activated electrons. In that case, THz photon detection by the device will depend on the polarization of THz wave. Otherwise, a THz wave will only heat electrons to broaden the resonance peak.

5 Conclusions

Reproducible THz photocurrents have been detected by a GaAs-based wrap-gate single electron transistor at low temperature. Analysis based on Tien-Gorden photon-assisted-tunneling theory shows that the THz photon energy could be characterized by the gate voltage spacing between the resonance peak and satellite peak. The temperature dependence of the resonance peak further verifies that the satellite peak is exactly generated by THz photons. Both experimental results and theoretical analysis show that the narrow spacing of double barriers is the most useful for the enhancement of THz response at higher temperature. Narrow gate length is also helpful for the increase of THz response. A future THz detector of a single electron transistor should consist of a very small quantum dot and very thin tunneling barriers.

References

[1] Tien P K, Gordon J P. Multiphoton process observed in the interaction of microwave fields with the tunneling between superconductor films. Phys Rev, 1963, 129(2): 647

[2] Sashinaka N, Oguma Y, Asada M. Observation of terahertz photon-assisted tunneling in triple-barrier resonant tunneling diodes integrated with patch antenna. Jpn J Appl Phys Part 1, 2000, 39(8): 4899

[3] Keay B J, Zeuner S, Allen S J Jr, et al. Dynamic localization, absolute negative conductance, and stimulated, multiphoton emission in sequential resonant tunneling semiconductor superlattices. Phys Rev Lett, 1995, 75(22): 4102

[4] Wyss R A, Eugster C C, del Alamo J A, et al. Far-infrared photon-induced current in a quantum point contact. Appl Phys Lett, 1993, 63(11): 1522

[5] Kouwenhoven L P, Jauhar S, Orenstein J, et al. Observation of photon-assisted tunneling through a quantum dot. Phys Rev Lett, 1994, 73 (25): 3443

[6] Komiyama S, Astafiev O, Antonov V, et al. Single-photon detection of THz-waves using quantum dots. Microelectron Eng, 2002, 63: 173

[7] Foxman E B, McEuen P L, Meirav U, et al. Effects of quantum levels on transport through a Coulomb island. Phys Rev, 1993, B47 (15): 10020

[8] Büttiker M, Landauer R. Traversal time for tunneling. Phys Rev Lett, 1982, 49 (23): 1739

[9] Hu Qing. Photon-assisted quantum transport in quantum point contacts. Appl Phys Lett, 1993, 62 (8): 837

GaAs基单电子晶体管低温探测THz光子的研究*

韩伟华[1,†] 汤圆美树[2] 葛西诚也[2]

(1 中国科学院半导体研究所 半导体集成技术工程研究中心，北京 100083)

(2 北海道大学集成量子电子学研究中心，札幌 060-8628，日本)

摘要： 低温条件下具有肖特基围栅结构的GaAs基单电子晶体管可重复探测到THz光子的光电流响应.实验表明，2.54THz的CH_3OH气体激光垂直入射到单电子晶体管的量子点上，在随栅压变化的源漏共振电流峰附近，产生附加电流峰.通过这两个峰位的栅压间距可以估算出THz光子的能量.这表明附加电流峰是由THz光子辅助电子隧穿产生的.实验和理论都表明，单电子晶体管量子点尺寸的减小有利于THz光电流信号的增强.

关键词： 单电子晶体管；THz光子探测；光子辅助隧穿

EEACC： 2560

中图分类号： TN321 **文献标识码：** A **文章编号：** 0253-4177(2007)04-0500-07

---

* 国家自然科学基金资助项目(批准号：60506017)

† 通信作者.Email：weihua@red.semi.ac.cn

2006-07-06收到，2006-12-07定稿

©2007 中国电子学会